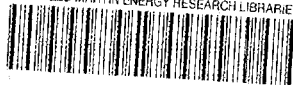
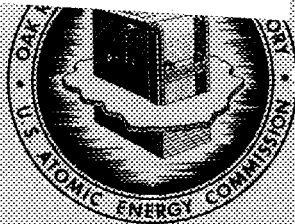


LOCKHEED MARTIN ENERGY RESEARCH LIBRARIES



3 4456 0514458 1



CENTRAL RESEARCH LIBRARY  
DOCUMENT COLLECTION

# OAK RIDGE NATIONAL LABORATORY

operated by

UNION CARBIDE CORPORATION • NUCLEAR DIVISION

for the

U. S. ATOMIC ENERGY COMMISSION



ORNL - TM - 3385

*cy. 1*

## OBSERVATIONS OF FUEL-CLADDING CHEMICAL INTERACTIONS AS APPLIED TO GCBR FUEL RODS

R. B. Fitts, E. L. Long, Jr., and J. M. Leitnaker

OAK RIDGE NATIONAL LABORATORY  
CENTRAL RESEARCH LIBRARY  
DOCUMENT COLLECTION

### LIBRARY LOAN COPY

DO NOT TRANSFER TO ANOTHER PERSON

If you wish someone else to see this  
document, send in name with document  
and the library will arrange a loan

**NOTICE** This document contains information of a preliminary nature and was prepared primarily for internal use at the Oak Ridge National Laboratory. It is subject to revision or correction and therefore does not represent a final report.

This report was prepared as an account of work sponsored by the United States Government. Neither the United States nor the United States Atomic Energy Commission, nor any of their employees, nor any of their contractors, subcontractors, or their employees, makes any warranty, express or implied, or assumes any legal liability or responsibility for the accuracy, completeness or usefulness of any information, apparatus, product or process disclosed, or represents that its use would not infringe privately owned rights.

ORNL-TM-3385

Contract No. W-7405-eng-26  
METALS AND CERAMICS DIVISION

OBSERVATIONS OF FUEL-CLADDING CHEMICAL INTERACTIONS  
AS APPLIED TO GCBR FUEL RODS

R. B. Fitts, E. L. Long, Jr., and J. M. Leitnaker

Paper  
Presented  
at the  
Conference on  
Fast Reactor Fuel Element Technology  
April 13-15, 1971  
Materials Science and Technology Division  
American Nuclear Society

JULY 1971

OAK RIDGE NATIONAL LABORATORY  
Oak Ridge, Tennessee  
operated by  
Union Carbide Corporation  
for the  
U.S. ATOMIC ENERGY COMMISSION

LOCKHEED MARTIN ENERGY RESEARCH LIBRARIES



3 4456 0514458 1



## CONTENTS

	<u>Page</u>
Abstract . . . . .	1
Introduction . . . . .	2
Fuel-Cladding Interface in Fuel Pins . . . . .	2
Morphology of Attack . . . . .	2
Microprobe Analysis of Reaction Zones . . . . .	6
Out-of-Reactor Studies . . . . .	9
Cladding Compatibility with Fuel and Fission Products . . . . .	9
Cladding Compatibility with Oxidizing Atmospheres . . . . .	11
Mechanisms of Cladding Attack and Material Transport . . . . .	15
Oxide Layers . . . . .	15
Grain Boundary Attack and In-Fuel Rivers . . . . .	21
Iodine Transport Mechanisms . . . . .	22
Liquid Phase Transport . . . . .	24
Mechanical Transport . . . . .	27
Conclusions . . . . .	27
Acknowledgment . . . . .	28
References . . . . .	29



OBSERVATIONS OF FUEL-CLADDING CHEMICAL INTERACTIONS

AS APPLIED TO GCBR FUEL RODS

R. B. Fitts      E. L. Long, Jr.      J. M. Leitnaker

ABSTRACT

Chemical interactions between fuel and cladding may be a major limitation to oxide-fueled fast breeder reactors. This limitation is especially important for long-term gas-cooled fast breeder reactor (GCBR) applications because of a strong economic incentive to operate at higher cladding temperatures. ORNL irradiation tests of (U,Pu)O<sub>2</sub> fuel pins clad in Hastelloy X and types 304 and 316 stainless steel show that the Hastelloy X cladding may be sufficiently compatible with mixed oxide fuels at 50 to 100°C higher. Out-of-reactor oxidation studies on type 316 stainless steel, conducted at ORNL, along with published information on oxidation of steels and in-reactor "fuel-cladding compatibility," are combined with a thermodynamic analysis of postulated reactions to yield the following conclusion. Most observations of fuel-cladding chemical interaction appear to be the result of simple oxidation of the cladding followed in some areas by mechanical or liquid-phase transport of the outermost oxide layer onto the fuel, where it is reduced. This conclusion indicates that, although type 316 stainless steel will be satisfactory for early GCBR application, either a more detailed understanding of the reaction involved is needed or alloys that are more oxidation resistant must be proven as cladding materials.

## INTRODUCTION

Chemical interactions between mixed oxide fuel, fission products, and cladding materials may be a major factor limiting the life of fuel rods in gas- and liquid-metal-cooled breeder reactors (GCBR and LMFBR). Fuel rods for early demonstration GCBR are designed<sup>1</sup> with type 316 stainless steel cladding to operate with a peak cladding hot-spot temperature of 700°C. With this design, the early GCBR and LMFBR fuel pins are very similar. For longer term applications there is an economic incentive to increase the coolant temperature in the gas-cooled system;<sup>1</sup> cladding performance at temperatures above 700°C and probably the performance of materials other than type 316 stainless steel then become important. We have examined in- and out-of-reactor tests at ORNL and the available literature for evidence of fuel-cladding chemical interaction and oxidation attack on cladding materials. Finally, some proposed mechanisms of cladding attack are discussed in the light of these observations and thermodynamic analysis of the postulated reactions.

## FUEL-CLADDING INTERFACE IN FUEL PINS

Morphology of Attack

Chemical interactions between mixed oxide fuel and cladding materials have been observed at ORNL in a number of fuel pins irradiated as part of a cooperative ORNL-GGA GCBR fuel development program<sup>2,3</sup> and as part of the ORNL Oxide Fuels Development program.<sup>4</sup> The fuel pins, listed in Table I, were clad with Hastelloy X or type 304 or 316 stainless steels. The cladding inner surface temperatures ranged from about 600 to 1000°C and the fuel burnups from 4,000 to 60,000 MWD/metric ton.

Table I. Data from Selected Irradiation Tests at ORNL

Test Pin Identifi- cation	Cladding			Fuel			Conditions				Reactor	
	Material	Penetra- tion (mils)	Surface Reaction Layer Thickness (mils)	Composition		Form <sup>b</sup>	Swear Density (%)	Heat Rating <sup>c</sup>	Burnup <sup>d</sup> (% FIMA)	Calculated Peak Cladding Inner Surface Temperature <sup>e</sup> (°C)		Time in Test (Effective Full Power Hours)
				Pu	O <sup>A</sup>							
				U+Pu	U+Pu							
GA-14	Hastelloy X	~ 4 <sup>e</sup>	f	0.12	2.00	P	85	18.0	0.4	850	1,100	ORR
GA-13	Hastelloy X	~ 2 <sup>e</sup>	f	0.12	2.00	P	85	15.8	0.4	810	1,100	ORR
GA-16	Hastelloy X	2 <sup>e</sup>	2	0.12	2.00	P	85	7.0	1.9	750	7,800	ORR
GA-18	Hastelloy X	0	2	0.12	2.00	P	85	15.2	6.3	710	10,250	ORR
GA-19	Hastelloy X	0	2	0.12	2.00	P	85	15.2	6.3	710	10,250	ORR
99-3	Type 304 stainless steel	0	0	0.20	2.00	S	76	49.9	2.8	1000	460	
99-1	Type 304 stainless steel	0	0	0.20	2.00	S	76	34.6	1.4	730	460	ETR
115-3	Type 304 stainless steel	0	0	0.15	2.00	S	82	20.6	6.5	460	4,180	ETR
GA-17	Type 316 stainless steel	0	2	0.12	2.00	P	85	12.2	5.1	580/630	10,250	ORR
S-1-B	Type 316 stainless steel	0	0	0.20	1.99	S	82	13.5	6.1	590	5,680	EBR-II

<sup>a</sup>Highest reported value; intended value usually lower

<sup>b</sup>S = Sphere-Pac; P = 90%-dense annular pellet.

<sup>c</sup>Time averaged.

<sup>d</sup>Fissions per initial metal atom.

<sup>e</sup>About 0.001 in. of grain boundary porosity, remainder open intergranular cracks in cladding.

<sup>f</sup>Intermittent, about 10- $\mu$ m-thick metallic and 2- $\mu$ m-thick oxide layers.

Hastelloy X cladding on (U,Pu)O<sub>2</sub> fuel at temperatures near 700°C, the lowest test temperature for this combination, shows a 0.002-in.-thick uniform reaction layer after relatively high burnup and long test duration (GA-18, -19). There was no measurable thinning of the cladding wall. At 750°C, lower burnup, and shorter times (GA-16), intergranular penetration of the cladding was observed as open "cracks" and, deeper in the cladding, grain boundary porosity. At temperatures above 750°C the extent of reaction increased; more voids were observed deeper in the cladding, and cladding thinning became measurable. The result of these reactions is shown in Fig. 1.

Our data from stainless-steel-clad fuel pins are limited but generally encouraging. In the single test of this type (GA-17) in which we saw cladding reaction we operated a pellet fuel to 5% FIMA at a peak cladding inside temperature of 630°C, and there was no measurable thinning of the cladding. The remainder of these tests were either below 600°C or for short times, and no attack was observed. This is most significant in the case of EBR-II fuel pin S-1-E, which achieved 6% FIMA at 590°C peak cladding inside temperature.

Other investigators have made numerous observations of attack at the inner surface of the cladding on mixed oxide fuel pins.<sup>5-7</sup> A definite effect of cladding inside temperature on the depth of cladding attack and probably a discernible effect of burnup (or irradiation time) have been reported.<sup>5,7</sup> An equation developed by Biancheria and coworkers<sup>8</sup> describing the available data on cladding penetration ( $\Delta t$ , mils) in terms of cladding surface temperature (T, °F) and fuel burnup (BU, MWd/metric ton) is

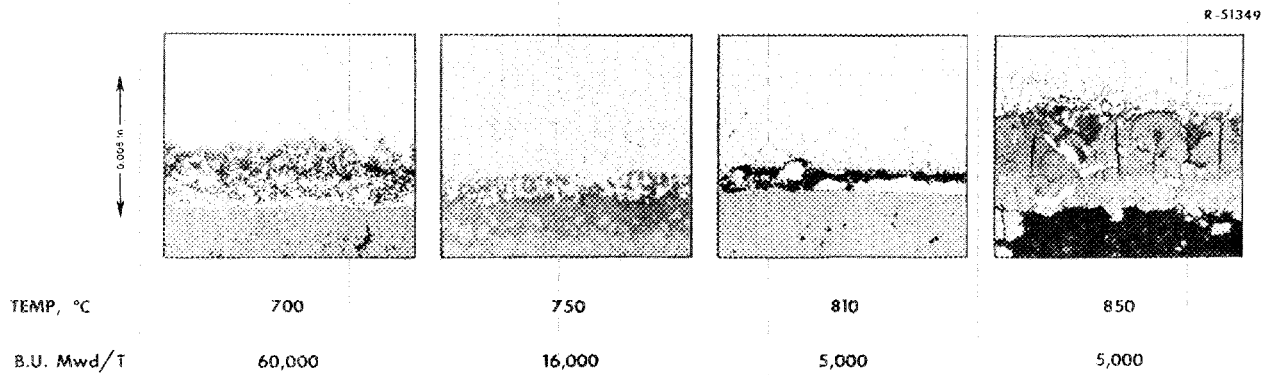


Fig. 1. Chemical Interaction Between Hastelloy X Cladding and  $(U,Pu)O_2$  in GCBR Fuel Pins. (a) 700°C, 60,000 MWd/metric ton, (b) 750°C, 16,000 MWd/metric ton, (c) 810°C, 5,000 MWd/metric ton, (d) 850°C, 5,000 MWd/metric ton.

$$\Delta t = 10^{-4} \text{ BU} \left[ 0.0426 + 5.6 \times 10^{-4} (T - 950) \right].$$

Unfortunately, the observations cannot be correlated well enough with any of the fuel rod fabrication or operating conditions to clearly define either the operative mechanisms or the kinetics of the reactions. Such a result is not surprising, in view of the very complicated nature of these tests and their analysis.

The overall appearance of the reaction zone is the same for both stainless steels and Hastelloy X. Three general forms of chemical reaction are observed. They are: (1) a layer of reaction product on the cladding inside surface (see Fig. 1); (2) grain boundary attack in the cladding (see Fig. 1); and (3) "rivers" of metallic material along cracks in the fuel (see Fig. 2). The relationship between these three forms of attack is not clear. However, the reaction layer located at the cladding surface is sometimes observed alone, whereas the penetration of grain boundaries in the cladding seems to occur only in combination with a layer of reaction product on the surface.

#### Microprobe Analysis of Reaction Zones

Information being collected at several sites with electron microprobe analyzers appears to be of most direct use in the analysis and understanding of the chemical reactions at the fuel-cladding interface. Some of the data of this type are summarized in Table II. As yet, the only distinct pattern apparent in these data is that oxides of the major constituents of the cladding are layered on its inner surface. The conditions under which intergranular penetration and "rivers" of metal in the fuel appear are not well defined. Temperatures above 600 to 650°C

R-49344

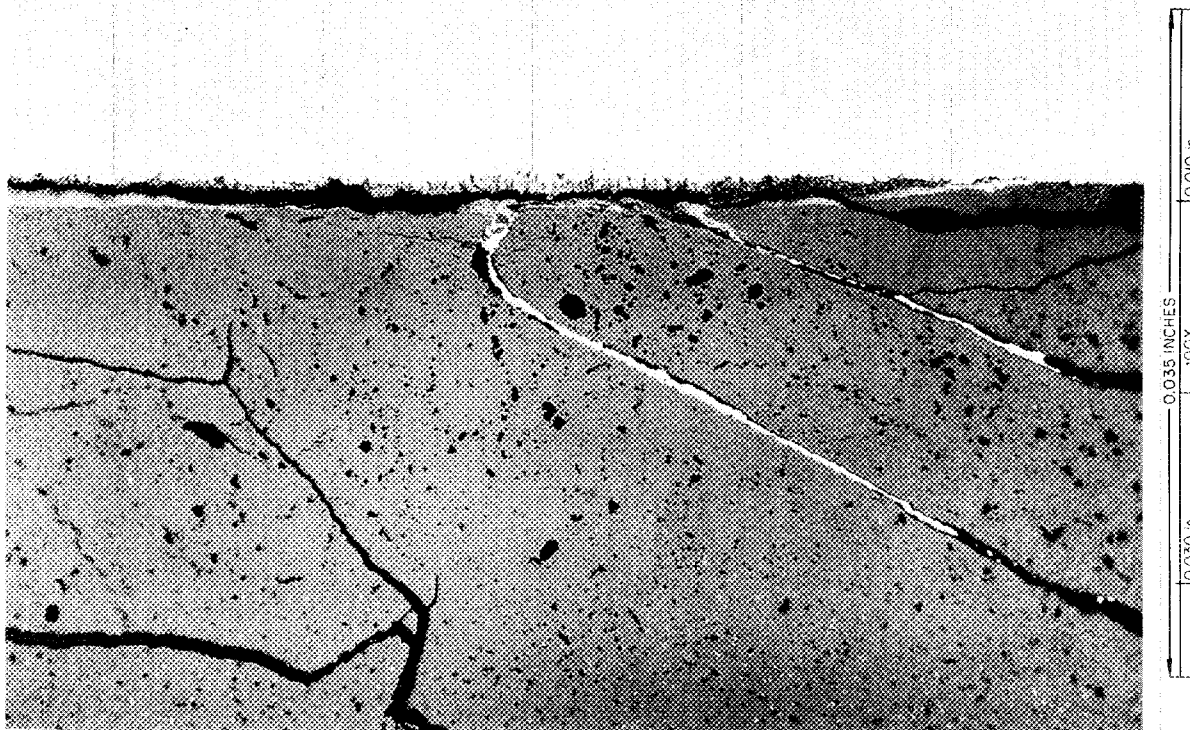


Fig. 2. Appearance of Metallic Rivers Observed in  $(U,Pu)O_2$  Fuel. The rivers apparently originated at the fuel-cladding interface. As polished. 100x

Table II. Selected Data from Electron Microprobe Analysis of Cladding Attack

Experiment	Cladding	Form	Fuel		Density (% of Theoretical)		Cladding Inside Temperature	Total Penetration (in.)	Constituents by Microprobe Analysis <sup>a</sup>			Ref.
			$\frac{\text{Pu}}{\text{U+Pu}}$	$\frac{\text{O}}{\text{U+Pu}}$	Fuel	Smear			in Grain Boundaries	in Reaction Layer	in Sivers	
SOV-6	304 SST	Vi-Pac	0.20	~ 2.00	83	83	650	0.003	Fe and Cr depletion, Ni enhancement, Cs	Cr + Cs	b	9
BNW-4-4I	304 SST	Pellet	0.25	1.96	93	87.5	665	b	No attack	(Mn + Cr)/Fe/Cr	Fe, <sup>c</sup> Ni, Cr, Mn	7
SOV-6	304 SST	Vi-Pac	0.20	~ 2.00	83	83	650	b	Si, Cs	b	b	10
F-2-H	316 SST	Pellet	0.20	1.98	97.5	95	540-580	b	No attack	Ni/Fe	b	11
F-12-C	316 SST	Pellet	0.25	1.97	87.5	83	705	0.004	Void	Cr/Ni/Fe/Cr (Ni/Fe (Cr) (Mo, Cs, Si)	b	12
F-12-D	316 SST	Vi-Pac	0.25	1.97	82.0	82	705	0.002	Si + Cs	(Fe + Ni)/Cr	b	12
F-2-C	Incoloy-800		0.20	2.00	95.5	93	NR	0.0005	No attack	Fe, Cr, Ni, Mn, Mo	b	13
GA-18	Hastelloy-X	Pellet	0.12	2.00	90	85	710	0.002	No attack	Cr/Ni/Fe Cr/(Ni + Fe)	Fe, trace Ni and Cr	—

<sup>a</sup>If the components are separated by a "slash," then they are listed in the order which they were observed, starting with the one nearest the cladding.

<sup>b</sup>Not reported.

<sup>c</sup>Major constituent.

00

in the stainless steels and 700 to 750°C in Hastelloy X seem to be required to produce intergranular penetration of the cladding.

We have examined by electron microprobe analysis at ORNL the "uniform" reaction layer on the Hastelloy-X-clad rod (GA-18), which operated at 710°C to 60,000 MWd/metric ton burnup. We found that the distribution of iron, nickel, and chromium through the reaction zone, as shown in Fig. 3, is quite similar to that observed in the surface layer on oxidized stainless steel (discussed below). The low point on each curve represents background level (there is no plutonium in the cladding). Microprobe analysis shows that the "rivers" in pins clad with either the Hastelloy X or stainless steel are predominantly iron with a trace of nickel and chromium sometimes present.

#### OUT-OF-REACTOR STUDIES

##### Cladding Compatibility with Fuel and Fission Products

Our-of-reactor studies of the compatibility of (U,Pu)O<sub>2</sub> fuel with cladding materials have shown<sup>14,15</sup> little or no fuel-cladding interaction except when the fuel was hyperstoichiometric. More recently, stainless steel cladding has been heated in the presence of fission product compounds,<sup>10,16</sup> (U,Pu)O<sub>2</sub> along with such compounds,<sup>13</sup> and UO<sub>2</sub> with such compounds.<sup>17</sup> In these experiments the effects of Cs, I, Sr, Ce, Te, and other fission products in hydroxide, oxide, chloride, and carbonate forms were studied. The only fission product found to seriously affect the stainless steel was cesium. It promotes intergranular attack, but this effect was strong only in the presence of oxygen.

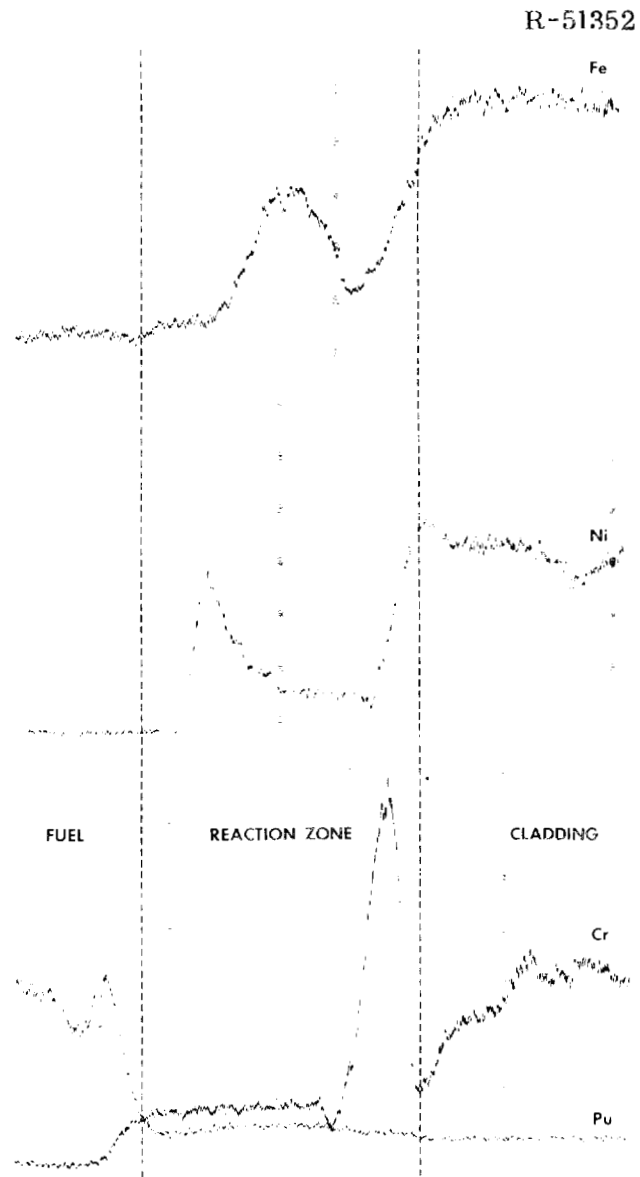


Fig. 3. Strip Chart Recording of X-Ray Scans Across Fuel-Cladding Interface by Electron Microprobe Analysis.

Cladding Compatibility with Oxidizing Atmospheres

Other relevant studies over the last decade relate to the oxidation of candidate cladding materials. Several studies of the oxidation of stainless steels and nickel-base alloys in various overpressures of  $\text{CO}_2$ <sup>17-20</sup> and  $\text{CO}_2 + \text{CO}$ <sup>21,22</sup> have shown oxidation phenomena very similar to the reaction layers and grain boundary attack observed in irradiated fuel pins.

In light of the above oxidation studies and the great similarity between this form of attack and the in-reactor problem,<sup>23</sup> we carried out an experimental oxidation heat treatment on a type 316 stainless steel tube. The inner and outer surfaces of the tube were exposed to flowing Ar-4%  $\text{H}_2$  containing a controlled amount of moisture ( $\sim 4000$  ppm) to simulate the oxidizing conditions to which the inside of such tubing is exposed when used for cladding on mixed oxide LMFBR-type fuel pins. A temperature gradient was imposed along the tubing during the heat treatment to provide, by appropriate selection of samples, metallographic observation of the oxidation layer developed at various temperatures. The heat treatment was held to 500 hr. A sample was also taken from a piece of similar tubing that had been held at  $925^\circ\text{C}$  for 500 hr with the outer surface exposed to air and the inner surface only to the controlled low-oxygen atmosphere.

The comparative results of the metallographic examination are shown in Figs. 4 and 5 and Table III. As can be seen in Fig. 4, there was no measurable attack in the low-oxygen atmosphere until about  $675^\circ\text{C}$  was reached. The attack was in the form of intergranular penetration of the cladding beneath an adherent oxide film. In fact, the appearance



(a)



(b)



(c)



(d)



(e)

Fig. 4. Appearance of Sections Along a Type 316 Stainless Steel Tube Oxidized in a Controlled Atmosphere for 500 hr. (a) 460°C, (b) 550°C, (c) 675°C, (d) 775°C, and (e) 900°C. As polished. 750X.

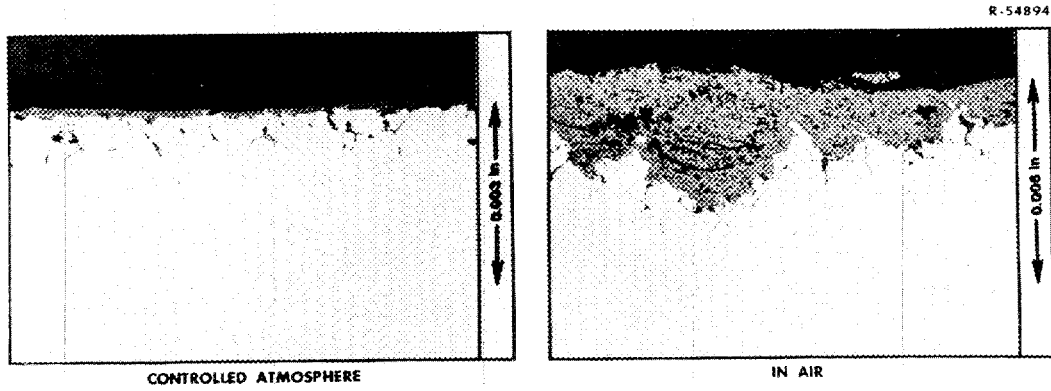


Fig. 5. Appearance of Oxide Scale and Intergranular Attack on Type 316 Stainless Steel Oxidized at 925°C for 500 hr.

Table III. Data from 500 hr Oxidation of Type 316 Stainless Steel

Temperature (°C)	Atmosphere	Reaction Depth-Max (μm)	
		Oxide Film	Intergranular Penetration
460	Low O <sub>2</sub> <sup>a</sup>	0	0
550	Low O <sub>2</sub> <sup>a</sup>	0	0
675	Low O <sub>2</sub> <sup>a</sup>	1.7	1.7
775	Low O <sub>2</sub> <sup>a</sup>	3.4	8.5
900	Low O <sub>2</sub> <sup>a</sup>	3.4	19
925	Low O <sub>2</sub> <sup>a</sup>	4.4	20
925	Air	75	25

<sup>a</sup> Ar-4% H<sub>2</sub> containing ~4000 ppm H<sub>2</sub>O.

of the attack at the higher temperatures bears a strong resemblance to attack at fuel-cladding interfaces.

The section from the tubing that was exposed to air is shown in Fig. 5(a); this section clearly demonstrates the fact that intergranular attack progresses ahead of the oxide. Note that, as shown in Table III, for the 900 to 925°C range the depth of intergranular attack apparently does not depend on either the oxygen potential in the atmosphere or the thickness of oxide scale formed.

Some of the results from electron microprobe analyses of the oxide scale and adjacent base metal are shown in Figs. 6, 7, and 8. Inspection of the chromium, nickel, and iron x-ray displays shows an enhancement of chromium in the thin oxide scale formed in the controlled atmosphere at 925°C. Two different types of oxide scale were found on the heavily oxidized sample that was at the same temperature but in air. As can be seen in Figs. 6 and 7, a zone adjacent to the base metal was rich in chromium, followed by a layer containing all three metals, and occasionally the second oxide layer was followed by a third layer that was rich in iron (Fig. 8). The relative iron, chromium, and nickel contents of two oxide scales are given in Table IV.

#### MECHANISMS OF CLADDING ATTACK AND MATERIAL TRANSPORT

##### Oxide Layers

The sequence of component distribution in the oxide layers on attacked cladding is not constant. Electron microprobe examination of the cladding reveals in some samples (see Fig. 3) a chromium-rich oxide adjacent to the cladding, with a nickel-rich oxide nearest the fuel and

R-54904

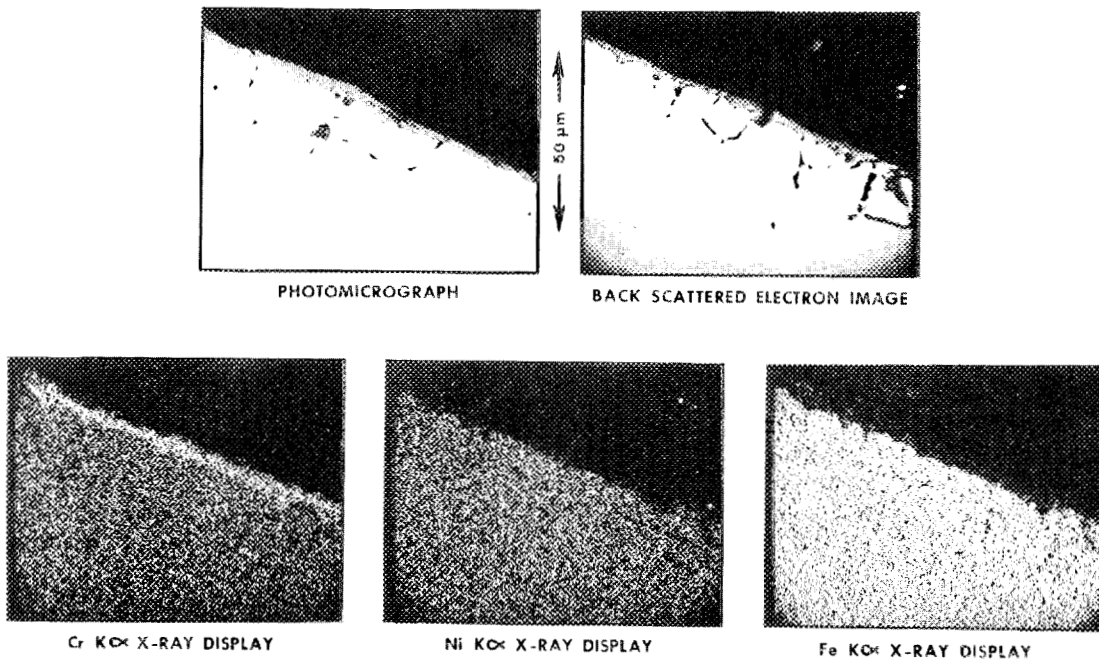


Fig. 6. Distribution of Chromium, Nickel, and Iron in an Oxide Layer Formed on 316 Stainless Steel in a Controlled Atmosphere at 925°C for 500 hr.

R-54902

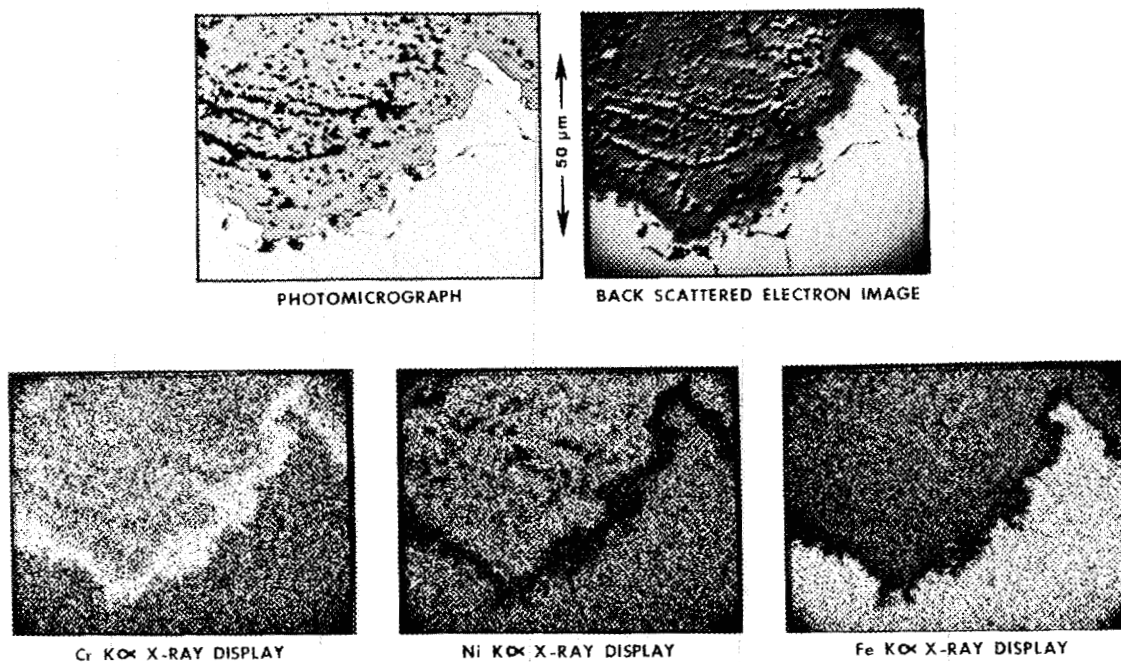


Fig. 7. Distribution of Chromium, Nickel, and Iron in Oxide Layers Formed on 316 Stainless Steel in Air at 925°C for 500 hr.

R-54903

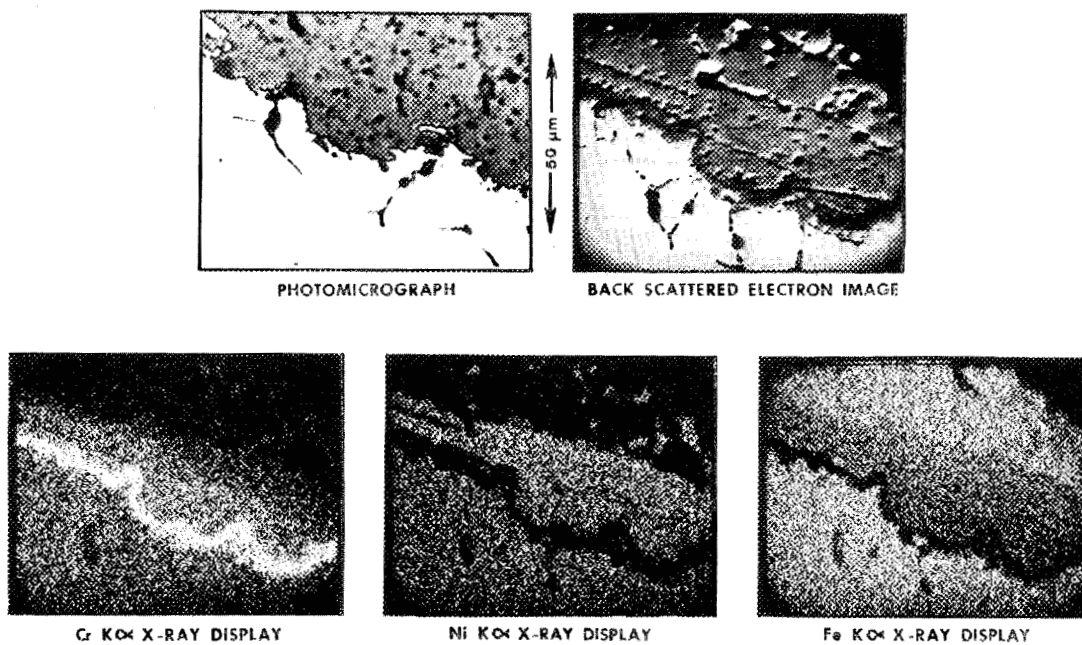


Fig. 8. Distribution of Chromium, Nickel, and Iron in Oxide Layers Formed on 316 Stainless Steel in air at 925°C for 500 hr. Region showing three distinct oxide layers.

Table IV. Electron Microprobe Analysis of Oxide Scales Formed on Type 316 Stainless Steel During Oxidation

Region Analyzed	Content, wt %		
	Fe	Cr	Ni
Thin scale <sup>a</sup>	10.5	87.2	2.3
Thin layer adjacent to cladding <sup>b</sup>	7.3	79.4	13.3
Middle oxide layer <sup>b</sup>	39.3	42.2	18.5
Outermost oxide layer <sup>b</sup>	69.7	30.1	0.3

<sup>a</sup>Thin oxide scale formed in low oxidizing atmosphere at about 925°C for 500 hr.

<sup>b</sup>Layered oxide scale formed in air at about 925°C for 500 hr.

an iron-rich phase between the two. In this case, the material behaves as if an oxygen lattice served as a chromatographic column with the least stable oxide moving the farthest and the most stable oxide moving the least. In other samples (see Table II) one finds exactly the reverse situation; chromium is more concentrated near the fuel while nickel is richest near the base metal. In still other samples the chromium is nearest the cladding but the iron has moved to a position nearest the fuel, with nickel in an intermediate position. Clearly, these differences in behavior indicate variations in the local environment in the experiment.

The cladding-Cr-Fe-Ni-fuel and cladding-Cr-Ni-Fe-fuel sequences are not uncharacteristic of oxidation in a high-oxygen environment. In the laboratory tests described above in which type 316 stainless steel was heated at 925°C for 500 hr in air, the same two sequences were seen (see Fig. 8 and Table IV). The reason for the difference is not known.

The sequence in irradiated fuel pins in which the chromium is near the fuel is more difficult to explain. A different mechanism of oxidation from that at high oxygen pressure seems indicated. Such a mechanism might involve fission products, such as cesium in some form. An alternate explanation could involve the fact that the chromium-rich layer formed at low oxygen potentials is not stable and can move by vaporization after long times at high temperature.<sup>19,22</sup> This mechanism, or mechanical spalling of the chromium-rich layer, would lead to oxidation of the newly exposed surface of the cladding. This surface has been depleted in chromium, and the formation of an iron-nickel oxide next to the cladding would result.

Grain Boundary Attack and In-Fuel Rivers

The depth of uniform and grain boundary attack observed in our out-of-reactor oxidation studies is generally consistent with that predicted for in-reactor fuel pins.<sup>7,8</sup> The 500-hr test duration is roughly equivalent to 5000 MWd/metric ton burnup in a GCBR or LMFBR fuel pin.

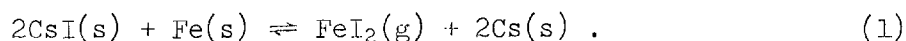
Two main factors have led to postulation of fission products as the primary culprits in fuel-cladding chemical interactions. One is the observation of fission products in the reaction layers and in the attacked grain boundaries of the cladding. Since those fission products so located normally move toward the cladding whether there is attack or not, their presence in the reaction zone is not proof that they are the attacking agent. The second factor taken to indicate fission product attack is the presence and composition of the metallic "rivers" in the fuel near the surface.

Speculation that the cladding is transported by an iodine mechanism similar to the Van Arkel-de Boer<sup>24</sup> process has resulted<sup>6,25</sup> from evidence such as that described above. Calculations from available thermodynamic data plus reasonable estimates show that such transport is impossible unless the participation of a stable cesium uranate is postulated. Moreover, even with this postulated mechanism, transport can only occur at relatively high oxygen potentials. More likely mechanisms are oxide transport through a liquid phase or mechanical transport. Calculations to demonstrate the above statements have been made as follows.

### Iodine Transport Mechanisms

The ratio of cesium formed to iodine formed in two years in a typical fast reactor is approximately six.<sup>26</sup> Thus, the iodine would tend to be tied up by the cesium as CsI as rapidly as the iodine is formed, so it would not be available in significant quantities to participate in transport of cladding components.

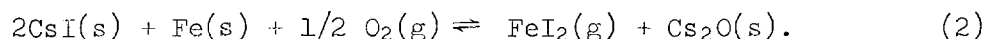
As a demonstration of the nonavailability of iodine, consider the reaction:



From data in Kubaschewski, Evans, and Alcock<sup>27</sup> plus an estimate of 30.0 e.u. for the entropy of vaporization of FeI<sub>2</sub>, one calculates the  $\Delta H_{298}^\circ$  of Reaction (1) as +167.7 kcal/mole and  $\Delta C_p$  between 298°K and the temperature of interest, can be taken as zero for the purposes of this calculation. Thus  $\Delta G^\circ/T$  is +146.5 cal mole<sup>-1</sup> (°C)<sup>-1</sup> at 900°K, and the pressure of FeI<sub>2</sub> at equilibrium would be about 10<sup>-32</sup> atm. Any significant transport of iron under these conditions is inconceivable.

However, other things are occurring in an oxide fuel pin. Specifically, the oxygen potential is changing. One might assume that the oxygen would tie up the cesium after a period of time, and then the pressure of iodine would begin to rise.

To examine this possibility, consider the reaction



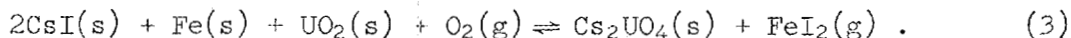
In this case  $\Delta H_{298}^\circ$  for the reaction is +91.6 kcal/mole and  $\Delta S_{298}^\circ$  is +4 e.u. At 900°K  $\Delta G^\circ/T$  is 97.8 and log K is -21.37. Since for

Reaction (2)  $K = \frac{P_{\text{FeI}_2}}{P_{\text{O}_2}^{\frac{1}{2}}}$ , one must know the pressure of oxygen to estimate the  $\text{FeI}_2$  pressures.

To find the influence of oxygen in Reaction (2), take the case of 900°K and an oxygen pressure of  $4 \times 10^{-15}$  atm. If oxygen at this temperature and pressure were in equilibrium with fuel, the oxygen-to-metal ratio would be 2.002 for a 20% Pu fuel.<sup>28</sup> Under these conditions, the pressure of  $\text{FeI}_2$  can be computed to be about  $3 \times 10^{-28}$  atm. It seems extremely unlikely that this mechanism could provide a significant transport, even allowing for any reasonable error in our basic assumptions.

Since the iron and sometimes other elements in the cladding are transported into the fuel and are observed as "rivers," some mechanism must be operable. Transport across the gap between the cladding scale and the fuel might occur either as a cyclical process or as a one-time transport. One must recognize that iron occurs almost pure (in some cases) and randomly located in the fuel pin, apparently as a "river" into the fuel from the fuel-cladding gap region. An acceptable overall mechanism must: (1) be thermodynamically possible, (2) explain why the iron occurs at only a few places, and (3) explain why the iron is separated from the other elements of the cladding.

If gas transport is possible within a fuel element then the participation of a cesium uranate might permit iron transport. Several cesium uranates are known. The compound  $\text{Cs}_2\text{UO}_4$  has a reported<sup>29</sup> heat of formation,  $\Delta H_{298}^\circ$ , of -478 kcal/mole, and we estimate an entropy,  $S_{298}^\circ$  of +51 e.u. The appropriate reaction is then

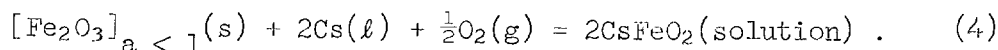


For Reaction (3)  $\Delta H_{298}^\circ$  is  $-51.5$  kcal. At  $900^\circ\text{K}$ ,  $\Delta G^\circ/T$  is  $-40.23$  and  $\log K$  is  $+8.791$ .

To see the effect of oxygen potential on Reaction (3), we chose the example used above ( $4 \times 10^{-15}$  atm  $\text{O}_2$  at  $900^\circ\text{K}$ ). In this case the pressure of  $\text{FeI}_2$  would be about  $3 \times 10^{-6}$  atm, clearly enough to provide a transport mechanism. On the other hand, at an oxygen-to-metal ratio of 2.00 the oxygen pressure is reduced so greatly that a  $\text{FeI}_2$  pressure of about  $10^{-16}$  atm is calculated.

### Liquid Phase Transport

Another possibility involving a cyclical process is formation and transport of a cesium ferrate across a liquid phase (such as cesium or  $\text{Cs}_2\text{O}$ ) between fuel and cladding. If one assumes that iron in the iron-rich phase near the fuel is in the +3 oxidation state, one can write,



For  $\text{CsFeO}_2$ ,  $\Delta H_{\text{f},298}^\circ$  is estimated to be  $-137.8$  kcal/mole and  $S_{298}^\circ$  is estimated at 30.0 e.u. Data for  $\text{Fe}_2\text{O}_3$  and cesium are taken from Kubaschewski, Evans, and Alcock.<sup>27</sup> The most favorable case is when  $a_{\text{Fe}_2\text{O}_3} = 1$ .

To examine this case a range of activities across a temperature gradient should be examined. Table V shows the computed range of activities of  $\text{CsFeO}_2$  from 1000 to 1500°K. To make the calculation for three of the cases, we assumed that  $P_{\text{O}_2}$  was fixed by a  $\text{CO}_2$ -CO mole ratio of 10; for the fourth case the  $P_{\text{O}_2}$  was assumed that in equilibrium over Fe-FeO. The activities are such that transport is conceivable by this mechanism. One must assume that the activities are linearly

related to the concentration and, thus, that the activity at the high-temperature end requires precipitation of the  $\text{CsFeO}_2$  from the super-saturated solution in cesium. In the first examples of Table V, the  $P_{\text{O}_2}$  is above the Fe-FeO equilibrium and FeO would be transported. In the last case the Fe-FeO equilibrium oxygen pressure is used. Enough activity is still present at 1500°K to justify the general argument.

Additional alkali metal-iron-oxygen compounds are known, such as  $\text{Na}_4\text{FeO}_3$ , in which the iron valence is +2. Such variations in compound type or valence should not change these conclusions. It is quite likely that iron exists not in the +3 state but in some lower valence. Conceptually, this situation can be visualized as having  $\text{Fe}_2\text{O}_3$  at a lower activity. The activities of the cesium ferrate would then be reduced by just the amount of the reduction of the iron oxide's activity. The mechanism depends only on having an activity at the hot side appreciably less than that at the cold side.

There are enough uncertainties in the estimates that transport by this mechanism represents a possibility. Separation of iron from nickel and chromium indicates a partitioning. One must postulate preferential attack of the cladding, an activity at the hot side greater than at the cold side, or dissolution of the nickel and chromium into the fuel.

If such a transport is assumed, one must further assume a mechanism to concentrate the iron into rivers. Surface diffusion is a possibility for such a mechanism. Further, iron is sometimes seen deposited on the surface of the fuel, as is chromium, and not agglomerated into rivers.

Table V. Calculated Activities of CsFeO<sub>2</sub> at Various Oxygen Pressures and Temperatures<sup>a</sup>

T (°K)	$\log_{10} P_{O_2}$ <sup>b</sup>	$\log_{10} a_{CsFeO_2}$ <sup>a</sup>
1000	-18.4	-1.16
1200	-13.5	-1.58
1500	- 8.7	-1.94
1500	-11.54	-2.65

<sup>a</sup>Reaction considered is  $Fe_2O_3(s) + 2Cs(l) + 1/2 O_2(g) \rightleftharpoons CsFeO_2(\text{solution})$ .

<sup>b</sup>The first three examples correspond to pressures of oxygen fixed by a CO<sub>2</sub>-CO mole ratio of 10.

### Mechanical Transport

A final possibility is the mechanical transport of iron oxide across the gap by abrasion during shutdown and startup, for example. Since iron occurs in conjunction with the fuel, the conclusion follows that the oxygen potential is below that in the Fe-FeO equilibrium region. Such a simple mechanical transport of oxide followed by reduction seems as probable as the other mechanisms.

### CONCLUSIONS

1. Three general forms of reaction are manifested in the cladding of (U,Pu)O<sub>2</sub> fuels: (1) surface oxide layer, (2) intergranular penetration of the cladding, and (3) "rivers" of cladding components in the fuel.
2. The location, frequency, and characterization of these reactions must be better described by investigators in this field for their results to be relevant to the early understanding and control of these phenomena.
3. The equation developed by Biancheria and coworkers to describe cladding attack appears to provide a reasonable fit to the widely scattered available data for stoichiometric and hypostoichiometric fuel.
4. The limited available in-reactor data are in agreement with out-of-reactor studies in indicating that Hastelloy X can operate 50 to 100°C higher than can types 304 and 316 stainless steel, without excessive fuel-cladding chemical interaction.
5. A Van Arkel-de Boer type mechanism for iodine transport of cladding components toward the fuel in operating fuel pins is thermodynamically very unlikely.

6. Although fission product compounds, particularly those of cesium, can attack cladding materials under the conditions prevailing in an operating (U,Pu)O<sub>2</sub> fast reactor fuel pin, the major form of cladding attack is probably oxidation. We have observed essentially the same morphology of cladding reaction in both out-of-reactor oxidation and in-reactor fuel pin tests.

7. It appears that the most likely sequence of events in cladding attack is (1) movement of cladding constituents into surface oxide phases by normal oxidation with the concurrent formation of grain boundary voids at the higher temperatures, (2) movement of the outer oxide layers to fuel surfaces or cracks by either mechanical or liquid-phase transport, and (3) subsequent reduction of the transported material to the metallic state at the fuel.

8. Type 316 stainless steel appears adequate for early GCBR application. However, for the higher temperatures and higher burnups required for the commercial GCBR, either better understanding and resultant control of cladding attack or alloys more resistant to attack will be required.

#### ACKNOWLEDGMENT

We would like to acknowledge the assistance of J. L. Miller, Jr., H. V. Mateer, T. J. Henson, and R. S. Crouse in the microprobe examination of the samples; L. G. Shrader and E. R. Boyd in the metallographic examinations; H. Inouye for his invaluable discussions of oxide scales formed on various steels and nickel-base alloys; R. A. Buhl for the execution of the stainless steel oxidation experiment; and W. J. Lackey,

T. N. Washburn, C. M. Cox, and A. R. Olsen for their encouragement and constructive criticism of this work.

## REFERENCES

1. P. FORTESCUE and W. I. THOMPSON, "GCFR Demonstration Plant Design," Proceedings of the Gas-Cooled Reactor Information Meeting at ORNL, April 27-30, 1970, CONF-700401, United States Atomic Energy Commission, Division of Technical Information Extension, pp. 795-811.
2. R. B. FITTS, J. R. LINDGREN, E. L. LONG, JR., and D. R. CUNEO, "Gas-Cooled Fast Reactor Fuel-Element Development," Proceedings of the Gas-Cooled Reactor Information Meeting at ORNL, April 27-30, 1970, CONF-700401, United States Atomic Energy Commission, Division of Technical Information Extension, pp. 864-878.
3. E. L. LONG, JR., F. R. McQUILKIN, D. R. CUNEO, J. R. LINDGREN, and J. N. SILTANEN, "Irradiation Testing of Fuel Rods Containing  $UO_2$  and  $(U,Pu)O_2$  for GCFR," pp. 179-184 in Ceramic Nuclear Fuels (International Symposium, May 3-8, 1969, Washington, D.C., sponsored by the Nuclear Division of the American Ceramic Society), ed. by O. L. Kruger and A. I. Kaznoff, American Ceramic Society, Columbus, Ohio, 1969.
4. C. M. COX, R. B. FITTS, A. R. OLSEN, and A. L. LOTT, "Irradiation Performance of Sol-Gel  $(U,Pu)O_2$  Fuels for Breeder Reactors," Symposium on Sol-Gel Processes and Reactor Fuel Cycles, Gatlinburg, Tenn., May 4-7, 1970, CONF-700502, United States Atomic Energy Commission, Division of Technical Information Extension, pp. 359-373.
5. K. J. PERRY and C. N. CRAIG, "Austenitic Stainless-Steel Compatibility with Mixed-Oxide Fuel," Trans. Am. Nucl. Soc., 12(2), 564-565 (1969).

6. C. JOHNSON, C. CROUTHAMEL, H. CHEN, and P. BLACKBURN, "Studies in Mixed Oxide Irradiated Fuels: Transport of Cladding Components," Trans. Am. Nucl. Soc., 12(2), 565-566 (1969).
7. J. W. WEBER et al., "Irradiation of Hypostoichiometric UO<sub>2</sub>-PuO<sub>2</sub> Fuel," Quarterly Progress Report April, May, June 1970, Reactor Fuels and Materials Development Program for Fuels and Materials Branch of USAEC Division of Reactor Development and Technology, August 1970, BNWL-1349-2, Battelle Northwest Laboratory, pp. 3.24-3.44.
8. A. BIANCHERIA, Westinghouse Advanced Reactors Division, Personal Communication, January 1971.
9. N. R. STALICA and C. A. SELLS, "Electron Microprobe Analysis of Irradiated Oxide Fuels," pp. 211-224 in Ceramic Nuclear Fuels (International Symposium, May 3-8, 1969, Washington, D.C., sponsored by the Nuclear Division of the American Ceramic Society), ed. by O. L. Kruger and A. I. Kaznoff, American Ceramic Society, Columbus, Ohio, 1969.
10. Sodium-Cooled Reactors Fast Ceramic Reactor Development Program, Thirty-Second Quarterly Report, August-October 1969, GEAP-10028-32 General Electric Advanced Products Division, p. 6.6.
11. Sodium-Cooled Reactors Fast Ceramic Reactor Development Program, Thirty-Fourth Quarterly Report, June 1970, GEAP-10028-34, General Electric Advanced Products Division, pp. 46-58.
12. Sodium-Cooled Reactors Fast Ceramic Reactor Development Program, Thirty-Fifth Quarterly Report, September 1970, GEAP-10028-35, pp. 49-60.
13. Sodium-Cooled Reactors Fast Ceramic Reactor Development Program, Thirty-Sixth Quarterly Report, December 1970, GEAP-10028-36, pp. 54-58.

14. T. LAURITZEN, Compatibility of Urania-Plutonia Fuels with Stainless Steel and Sodium, GEAP-5633, General Electric Advanced Products Operation (June 1968).
15. F. M. SMITH, Compatibility of Both Mixed Uranium-Plutonium Oxides and Nitrides with Sodium and 304-Stainless Steel, BNWL-1101, Pacific Northwest Laboratory (May 30, 1969).
16. Sodium-Cooled Reactors Fast Ceramic Reactor Development Program, Thirty-Fourth Quarterly Report, June 1970, GEAP-10028-34, General Electric Advanced Products Operation, pp. 58-60.
17. P. HOFMANN, F. THÜMLER, and H. WEDEMEYER, Compatibility Studies With Simulated Fission Products on Stainless Steel and Molybdenum, With and Without Presence of UO<sub>2</sub>, EURFNR-685 (KFK-979, Gesellschaft für Kernforschung mbH) (May 1969).
18. H. J. PESSL, Evaluation of Iron and Nickel Base Alloys for Medium and High Temperature Applications, HW-67715, General Electric Company (February 1961).
19. J. C. BOCKROS and W. P. WALLACE, The Oxidation of Metals by CO<sub>2</sub> at Temperatures of 1100-1740°F and Pressures of 1000-2000 psi, GA-700, General Atomic (March 25, 1959).
20. A. DRAYCOTT and R. SMITH, Initial Results on the Compatibility of Austenitic Stainless Steels with Carbon Dioxide, AAEC/E52 (1960).
21. J. C. BOCKROS and H. E. SCHOEMAKER, Reactor Materials Compatibility with Impurities in Helium, GA-1508, General Atomic (January 12, 1961).
22. H. INOUE, "High-Temperature Reactions of Type 304 Stainless Steel in Low Concentrations of Carbon Dioxide and Carbon Monoxide," Corrosion of Reactor Materials, International Atomic Energy Agency, Vienna, 1962.

23. W. V. CUMMINGS, H. S. ROSENBAUM, and R. C. NELSON, "Analysis of Irradiated Materials Using a Shielded Electron Microprobe Analyzer," Paper presented at the American Nuclear Society National Topical Meeting on Remote Handling and Examination in the Fast Reactor Field, Idaho Falls, Idaho, March 11-13, 1969.
24. A. E. VAN ARKEL and J. H. de Boer, Z. Anorg. Chem., 148, 345 (1925).
25. C. E. JOHNSON and C. E. CROUTHAMEL, J. Nucl. Mater., 34, 101-104 (1970).
26. K. E. SPEAR and J. M. LEITNAKER, Fuels and Materials Development Program Quart. Progr. Rept. Dec. 31, 1968, ORNL-4390, Oak Ridge National Laboratory, p. 46.
27. O. KUBASCHEWSKI, E. L. EVANS, and C. B. ALCOCK, Metallurgical Thermochemistry, 4th ed., Pergamon Press, London (1967).
28. K. E. SPEAR, A. R. OLSEN, and J. M. LEITNAKER, Thermodynamic Applications to (U,Pu)O<sub>2±x</sub> Fuel Systems, ORNL-TM-2494, Oak Ridge National Laboratory (1969).
29. E. A. IPPOLITOVA, D. G. FAUSTOVA, and V. I. SPITSYN, "Determination of Enthalpies of Formation of Monouranates of Alkali Elements and Calcium," pp. 170-172 in Investigations in the Field of Uranium Chemistry, ANL-trans-33, Division of Technical Information, United States Atomic Energy Commission (November 1964).

## INTERNAL DISTRIBUTION

1-3.	Central Research Library	158-160.	M. R. Hill
4.	ORNL - Y-12 Technical Library	161.	F. J. Homan
	Document Reference Section	162.	H. Inouye
5-14.	Laboratory Records Department	163.	W. J. Lackey
15-134.	Laboratory Records (FREP)	164-168.	J. M. Leitnaker
135.	Laboratory Records, ORNL RC	169-173.	E. L. Long, Jr.
136.	ORNL Patent Office	174.	A. L. Lotts
137.	R. E. Adams	175.	E. J. Manthos
138.	G. M. Adamson, Jr.	176.	W. R. Martin
139.	R. E. Blanco	177.	H. V. Mateer
140.	E. E. Bloom	178.	H. E. McCoy, Jr.
141.	R. A. Bradley	179.	C. J. McHargue
142.	R. A. Buhl	180.	J. L. Miller, Jr.
143.	J. A. Conlin	181.	A. R. Olsen
144.	C. M. Cox	182.	P. Patriarca
145.	R. S. Crouse	183.	W. H. Pechin
146.	F. L. Culler	184.	J. L. Scott
147.	D. R. Cuneo	185.	J. D. Sease
148.	J. E. Cunningham	186.	V. J. Tennery
149-153.	R. B. Fitts	187.	D. B. Trauger
154.	B. Fleischer	188.	T. N. Washburn
155.	J. H. Frye, Jr.	189.	A. M. Weinberg
156.	G. H. Goode	190.	J. R. Weir, Jr.
157.	W. O. Harms		

## EXTERNAL DISTRIBUTION

191. W. E. Baily, General Electric, BRDO, Sunnyvale, CA 94086

192. C. J. Baroch, Babcock & Wilcox, P.O. Box 1260, Lynchburg, VA 24505

193. D. F. Cope, RDT, SSR, AEC, Oak Ridge National Laboratory

194. E. A. Evans, WADCO, P.O. Box 1970, Richland, WA 99352

195. J. Green, Los Alamos Scientific Laboratory, P.O. Box 1663, Los Alamos, NM 87544

196. T. Iltis, RDT, SSR, AEC, Westinghouse, ARD, P.O. Box 154, Madison, PA 15663

197. D. L. Keller, Battelle Memorial Institute, 505 King Ave., Columbus, OH 43201

198. E. E. Kintner, RDT, AEC, Washington, DC 20545

199. P. J. Levine, Westinghouse, ARD, Waltz Mill Site, P.O. Box 158, Madison, PA 15663

200. C. L. Matthews, RDT, AEC, Oak Ridge National Laboratory

201. P. Murray, Westinghouse, ARD, Waltz Mill Site, P.O. Box 158, Madison, PA 15663

202. M. V. Nevitt, Argonne National Laboratory, 9700 South Cass Ave., Argonne, IL 60439

203. E. C. Norman, RDT, AEC, Washington, DC 20545

204. H. Pearlman, Atomics International, P.O. Box 309, Canoga Park,  
CA 91304
205. W. E. Ray, Westinghouse, ARD, Waltz Mill Site, P.O. Box 158,  
Madison, PA 15663
206. S. Rosen, RDT, AEC, Washington, DC 20545
207. P. G. Shewman, Argonne National Laboratory, 9700 South Cass Ave.,  
Argonne, IL 60439
208. S. Siegel, Atomics International, P.O. Box 309, Canoga Park,  
CA 91304
209. J. M. Simmons, RDT, AEC, Washington, DC 20545
210. A. A. Strasser, United Nuclear Corporation, Grasslands Rd.,  
Elmsford, NY 10523
211. C. E. Weber, RDT, AEC, Washington, DC 20545
212. G. A. Whitlow, Westinghouse, ARD, Waltz Mill Site, P.O. Box 158,  
Madison, PA 15663
213. Laboratory and University Division, AEC, Oak Ridge Operations
- 214-215. Division of Technical Information Extension